Acta Nat. Sci. (2024) 5(1): 1-10
DOI: 10.61326/actanatsci.v5i1.1
e-ISSN: 2718-0638

Original Research Paper
info@actanatsci.com
www.actanatsci.com

ACTA NATURA ET SCIENTIA PRENSİP

Calculation of Isothermal Compressibility and Bulk Modulus as a Function of Pressure in a Perovskite-Like Framework of $[(C_3H_7)_4N]$ $[Mn(N(CN)_2)_3]$

Sedat Avcı[1]✉ • Mustafa Kurt[2]

[1] Çanakkale Onsekiz Mart University, Çanakkale Applied Sciences Faculty, Department of Energy Management, 17100, Çanakkale, Türkiye, sedat.avci@comu.edu.tr
[2] Çanakkale Onsekiz Mart University, Engineering Faculty, Department of Electric-Electronic Engineering, 17100, Çanakkale, Türkiye, mkurt@comu.edu.tr

✉ Corresponding Author: sedat.avci@comu.edu.tr

Please cite this paper as follows:
Avcı, S., & Kurt, M. (2024). Calculation of Isothermal Compressibility and Bulk Modulus as a Function of Pressure in a Perovskite-Like Framework of $[(C_3H_7)_4N]$ $[Mn(N(CN)_2)_3]$. *Acta Natura et Scientia*, *5*(1), 1-10. https://doi.org/10.61326/actanatsci.v5i1.1

ARTICLE INFO

Article History
Received: 06.12.2023
Revised: 04.01.2024
Accepted: 08.01.2024
Available online: 22.05.2024

Keywords:
Perovskite-like frameworks
Structural phase transition
Grüneisen value
Bulk modulus
Isothermal compressibility

ABSTRACT

The many distortions in solid material that are most easily triggered by factors like pressure are called its structural degrees of freedom. Zeolites, perovskites, coordination polymers and metal-organic frameworks (MOFs) are all members of the extensive and significant family of solids known as framework materials. In the last decade, it has been shown that perovskite-like framework materials have great potential applicable in solar panel cell production. The Perovskite-like framework, $[(C_3H_7)_4N][Mn(N(CN)_2)_3]$ ($[TPrA][Mn(dca)_3]$, in short), has recently attracted scientists, due to its magnetism, ferroelectricity, luminescence, switchable dielectric behaviour, multiferroic behaviour, non-linear optical properties and also photovoltaic properties. Exerted pressure causes changes in the structural, optical, and electronic properties of perovskite and perovskite-like compounds. As a result of these effects, these compounds present phase transitions at certain pressures. The $[TPrA][Mn(dca)_3]$ compound also exhibits two structural phase transitions at 0.3 GPa and 3.0 GPa pressure. In this study, we calculated some important thermodynamic parameters, which are the isothermal Grüneisen value, isothermal compressibility, and Bulk modulus, as a function of pressure to analyse phase transition dynamics by using observed volume and frequency values from the literature. The Bulk modulus values were determined at 9.86 GPa for the Pcnb -phase and 36 GPa for the P21/n -phase by using calculated isothermal compressibility values. Our results confirm that the perovskite-like $[TPrA][Mn(dca)_3]$ compound is a good candidate for solar panel cell production, as corroborated in the literature.

INTRODUCTION

Researchers working on solar panel cell technologies face the challenge of fulfilling the growing worldwide demand for renewable energy and implementing sustainable technologies. To handle this challenge, they are striving to develop new compounds and to improve the power conversion efficiency of photovoltaic (PV) systems while also reducing their operational costs. Within a period of less than a decade, solar cell power conversion efficiencies have reached up to 25% by using perovskite materials as raw materials in the production of solar cells, exceeding that of thin film or multi-layer silicon (Min et al., 2021; Jošt et al., 2022). In addition to the usage of perovskite compounds in PV technologies, scientists and engineers are finding new materials having perovskite and perovskite-like structure attractive because of its intriguing features and potential usage in electrical, optical, and energy storage systems (Grinberg et al., 2013; Shen et al., 2015; Wang et al., 2015). Recent studies have shown that perovskite-like frameworks of $[(C_3H_7)_4N][Mn(N(CN)_2)_3]$ (abbreviated as $[TPrA][Mn(dca)_3]$) exhibit properties similar to perovskites compounds (Mączka et al., 2019). The size and shape of the organic cation, the length and flexibility of the molecular linker, as well as its capacity to form hydrogen bonds with the metal linker framework, all have an impact on the crystal structures and properties of molecular perovskites (Huang et al., 2017; Assirey, 2019; Li et al., 2019). Pressure is one of the main parameters used to manipulate and control the electronic structure and behaviour of perovskite solar cells in the production processes (Oyelade et al., 2020). Molecular crystals, such as perovskites and perovskite-like frameworks, undergo structural phase transitions as the pressure increases, resulting in changes in molecular order. Hence, comprehending the mechanisms behind the phase transition of these types of compounds is highly intriguing, both from the standpoint of crystal engineering and because of their prospective applications. The applicability of $[TPrA][Mn(dca)_3]$ in solar panel cell manufacture can be greatly improved by controlling the structural phase transition that occurs under different pressure settings during the production processes (Bermúdez-García et al., 2015; Agyei-Tuffour et al., 2016, 2017). The Perovskite-like framework $[TPrA][Mn(dca)_3]$ exhibits two structural phase transitions depending on applied pressure. The first transition occurs from tetragonal phase ($P\text{-}42_1c$) to orthorhombic phase (Pcnb) at 0.3 GPa, and the second transition occurs from orthorhombic phase (Pcnb) to monoclinic phase (P21/n) at 3.0 GPa and ambient temperature (Bermúdez-García et al., 2015, 2017a; Mączka et al., 2019). Although there are previous studies related to pressure-induced structural phase transitions, there is currently a lack of comprehensive investigations that adequately clarify the micro dynamics of the phase transition in $[TPrA][Mn(dca)_3]$.

In this work, we calculated the Grüneisen value (γ_T), compressibility (κ), and Bulk modulus by using pressure dependent observed internal Raman and IR modes ($\nu_s(C\equiv N)$, $\nu_{as}(C\equiv N)$, $\delta(CNC)$, $\varrho(CH_2)$ and T(dca)+L(dca)+T(Mn)) in $[TPrA][Mn(dca)_3]$ for $P\text{-}42_1c$, Pcnb and $P2_1/n$ phases as a function of pressure. By using Grüneisen and Einstein approximations for frequency of soft modes in molecular crystals, we also calculated the frequency of the interested modes as a function of pressure and compared the calculated value and observed value to the Raman and IR mode frequencies in [TPrA][Mn(dca)3] given by Mączka et al. (2019).

MATERIAL AND METHODS

Thermodynamics provide a fundamental scientific framework in engineering and basic sciences, although its practical implementation across several fields has given rise to distinct variations characterized by specific terminology and notation. One of the most familiar parameters that is used to define how a crystal lattice's size or dynamics modify under pressure or at a certain temperature in thermodynamics is the Grüneisen value (γ). This parameter is a dimensionless thermodynamic quantity that is named after the German scientist Eduard Grüneisen. Its initial description was established in relation to the nonlinearities of phonons (Grüneisen, 1912). The Grüneisen value can also be defined as an observable thermodynamic parameter in a microscopic model that describes the vibrational

behaviour of atoms within a crystal lattice. Einstein demonstrated that the quantum harmonic oscillator, which represents a mode of crystal vibration in his theory, exhibits a relationship between the frequency of the mode and volume dependence. This relation is characterized by Grüneisen parameter, which can be expressed as a straightforward combination of well-known thermal and mechanical properties (Stacey & Hodgkinson, 2019). Whether the recalling force acting on an atom displaced from its primary position is or is not linearly dependent on the displacement, the frequency of phonons in the crystal will change in association with variations in the crystal's volume. The phenomenon can be used to establish a correlation between the Grüneisen value and the frequency shift of Raman modes by the anharmonic approximation. As mentioned by Stacey & Hodgkinson (2019) and Kurt's (2022) works, the average total energy in an atom is defined as:

$$E = \sum_{n=0}^{\infty} E(n) = \frac{h\nu}{\left[exp(\frac{h\upsilon}{kT})-1\right]} \quad (1)$$

The energy is equivalent to the thermal energy associated with a singular mode in the oscillation of a crystal, characterized by natural frequency and denoted as ν. This frequency is dependent on the volume variation of the crystal, as described in Einstein's theory (Einstein, 1907). Eq. (1) derived from Einstein's model for crystal structure is fundamental to Grüneisen's theory. The Isothermal Grüneisen value corresponding to each Raman or IR internal mode in atomic crystals can be defined as (Stacey & Hodgkinson, 2019):

$$\gamma_T = -\frac{d\, ln\, \upsilon_i}{d\, ln\, V} \quad (2)$$

where υ_i is the frequency for i^{th} mode in a crystal and V is the volume at constant temperature. From here the Grüneisen value is derived at constant temperature γ_T as a function of pressure:

$$\gamma_T = -\frac{V}{\nu}\frac{(\partial\nu/\partial P)_T}{(\partial V/\partial P)_T} \quad (3)$$

where ν is the frequency of Raman or IR internal mode as a function of pressure and V is the volume of a molecular crystal as a function of pressure, under constant temperature T. To calculate the frequency value as a function of pressure for each mode in a molecular crystal, Eq. (2) is integrated. Then frequency is calculated as:

$$\upsilon_T = \upsilon_0\, exp\left[-\gamma_T\, ln\left(\frac{V_T(P)}{V_0}\right)\right] + Const. \quad (4)$$

Eq. (4) includes volume that is dependent on pressure, so an equation for volume as a function of pressure was then derived. Findings of Mączka et al. (2019) for [TPrA][Mn(dca)$_3$] showed that volume exhibit a parabolic variation tendency while pressure is increasing. Therefore, a second-order polynomial function for the observed volume data of the molecular crystal [TPrA][Mn(dca)$_3$] was used in our calculations, as also used previously by scientist in the literature (Yurtseven & Kurt, 2011; Yurtseven & Cebeci, 2015; Yurtseven & Ünlü, 2015; Kurt, 2020):

$$V_T(P) = a_o + a_1 P + a_2 P^2 \quad (5)$$

where the coefficients a_o, a_1 and a_2 are constants at ambient temperature. In order to determine these coefficients, Eq. (5) was fitted to volume data from the literature (Mączka et al., 2019), as shown in Figure 1 and Table 1 for [TPrA][Mn(dca)$_3$]. The volume data of this compound showed discontinuity in the vicinity of 0.3 and 3 GPa pressure. These pressure values also corresponded to the structural phase transition from P-42$_1$c to Pcnb and from Pcnb to P2$_1$/n, respectively.

Table 1. The coefficients of Eq. (5), determined by fitting to the experimental volume data (Mączka et al., 2019) for P-42$_1$c, Pcnb and P2$_1$/n phases in [TPrA][Mn(dca)$_3$].

Phase	a_0 (A^0)^3	$-a_1$ ((A^0)^3/ GPa)	a_2 ((A^0)^3/ GPa^2)	V_0 (A^0)^3
P-42$_1$c	4621.95	467.43	-198.33	4621.95
Pcnb	4507.31	412.72	57.12	4507.31
P2$_1$/n	4088.01	111.98	1.65	4088.01

Table 2. The coefficients of Eq. (6), determined by fitting to the experimental frequency data (Mączka et al., 2019) for ν_s(C≡N), ν_{as}(C≡N), δ(C-NC), ϱ(CH2) and T(dca)+L(dca)+T(Mn) internal modes for P-42$_1$c, Pcnb and P2$_1$/n phases in [TPrA][Mn(dca)$_3$].

	Mode	T(dca)+ L(dca)+ T(Mn)	ϱ(CH$_2$)	δ(CNC)	ν_{as}(CN)	ν_s(CN)
Pcnb	b_0 (cm^{-1})	178.37	773.84	846.78	2159.82	2244.96
	b_1 (cm^{-1}/GPa)	11.08	9.03	10.53	7.65	3.80
	-b_2 (cm^{-1}/GPa^2)	1.27	0.93	1.13	0.37	-0.41
	ν_0 (cm^{-1})	178.37	773.84	846.78	2159.82	2244.96
P2$_1$/n	b_0 (cm^{-1})	198.53	772.46	864.57	2183.73	2251.94
	b_1 (cm^{-1}/GPa)	3.65	7.41	-0.22	-2.44	2.84
	b_2 (cm^{-1}/GPa^2)	0.08	-0.31	0.46	0.70	-0.07
	ν_0 (cm^{-1})	198.53	772.46	864.57	2183.73	2251.94

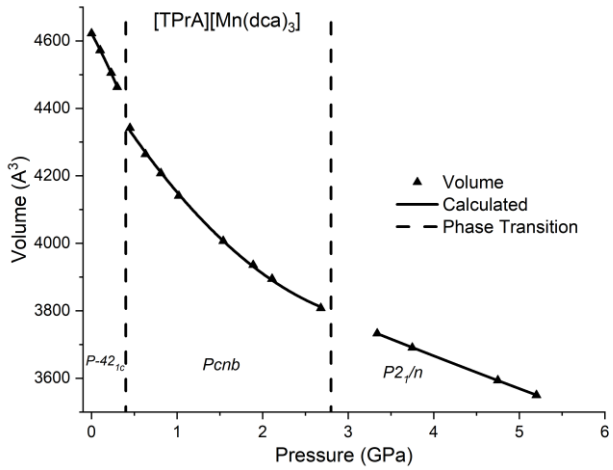

Figure 1. Calculated and observed (Mączka et al., 2019) volume data for P-42$_1$c, Pcnb and P2$_1$/n phases in [TPrA][Mn(dca)$_3$].

Eq. (3) also contains a frequency function that is dependent of pressure. In addition, the observed Raman modes data of ν_s(C≡N), ν_{as}(C≡N), δ(CNC), ϱ(CH$_2$) and T(dca)+L(dca)+T(Mn) for [TPrA][Mn(dca)$_3$] showed a parabolic change with pressure. The frequency of the Raman and IR internal modes in [TPrA][Mn(dca)$_3$] was defined as a second-order polynomial depending on pressure, like the volume function (Eq. 5). To obtain frequency as a function of pressure, the experimental data was iterated to the following equation:

$$\nu_T(P) = b_o + b_1 P + b_2 P^2 \quad (6)$$

where b_0, b_1 and b_2 are constants. In order to determine these constants for each Raman mode including ν_s(C≡N), ν_{as}(C≡N), δ(C-NC), ϱ(CH$_2$) and T(dca)+L(dca)+T(Mn), the experimental data taken from the literature (Mączka et al., 2019) were fitted to Eq. (6) for each phase in [TPrA][Mn(dca)$_3$], as shown in Figure (2) and presented in Table 2. Subsequently, the isothermal Grüneisen values from 0 to 6 GPa for the interested Raman and IR Modes in [TPrA][Mn(dca)$_3$] were determined with Eq. (4) through the calculated volume and frequency with the coefficients (presented in Tables 1 and 2) derived from the experimental data, which varied as a function of pressure, as shown in Figure 3.

Compressibility and bulk modulus are also very important thermodynamic parameters needed to understand the thermoelastic and thermodynamic properties and behaviour of solids under high pressure and temperature, like the Grüneisen parameter. Compressibility (defined as "isothermal compressibility" at constant temperature) refers to the extent to which a fluid or solid changes its volume in response to a change in pressure or mean stress in thermodynamics. The Isothermal Compressibility relation is very well known in thermodynamics and is expressed as follows:

$$\kappa_T = -\left(\frac{1}{V}\right)\left(\frac{\partial V}{\partial P}\right)_T \quad (7)$$

where V is volume and P is pressure at constant temperature. Defining compressibility with a negative sign ensures that compressibility is positive when an increase in pressure leads to a decrease in volume. The isothermal compressibility can be related to the internal mode of molecular crystals by deriving from Eq. (3) and (7) as in the following equation:

$$\kappa_T = \frac{1}{\gamma_T}\frac{1}{v}\left(\frac{\partial v}{\partial P}\right) \quad (8)$$

By using Eq. (8), the isothermal compressibility for [TPrA][Mn(dca)$_3$] from 0 GPa to 6 GPa at constant temperature can be calculated, as shown in Figure 4. The bulk modulus refers to the proportion of the rise in pressure related to the subsequent decrease in volume of a material and describes the degree of resistance of a substance to compression. Moreover, the bulk modulus is known as a measure of elastic characteristics due to its ability to return a compressed material to its initial volume under zero pressure. The relationship between compressibility and bulk modulus can be expressed as:

$$\beta = \frac{1}{\kappa} \quad (9)$$

The bulk modulus of [TPrA][Mn(dca)$_3$] for Pcnd and P2$_1$/n phases was calculated for pressures between 0 to 6 GPa by utilizing the calculated values of isothermal compressibility, as shown in Figure 5. The intercept and slope of the bulk modulus for both phases is also presented in Table 3.

Table 3. Intercept (K_0) and slope (K_0'), determined by fitting calculated Bulk modulus for P-42$_1$C, Pcnb and P2$_1$/n phases in [TPrA][Mn(dca)$_3$].

Phase	K_0 (GPa)	K_0'	Pressure Interval (GPa)
Pcnb	9.89	4.95	0.3<P<2.5
P2$_1$/n	36.07	0.26	3.0<P<6

RESULTS AND DISCUSSION

Pressure is an important parameter that can be employed to manipulate the electrical configuration and characteristics of organic-inorganic perovskite solar cells in production process es (Xiao et al., 2017). Exerting pressure on perovskite results in the compression of molecules. This leads to a higher degree of packing and a decrease in the distances between atoms, ultimately altering the electronic orbitals and bonding configurations. Therefore, applying pressure on perovskites in the production processes can cause alterations in the structural, optical, magnetic, and electrical characteristics of both organic and inorganic perovskite compounds (Huang et al., 2017). Applying pressure can enhance the interlayer contact inside solar cell designs (Tan & Cheetham, 2011; Xiao et al., 2014). By acquiring insight into the impact of pressure on the layers of organic-inorganic perovskite compounds, material properties can be adjusted by relating to compression. Studies related to characteristics of organic-inorganic perovskite under high pressure serve as a guiding framework for the subsequent design, synthesis, and application of materials with the structure and/or features of these perovskites (Oyelade et al., 2020).

For the current study, first the frequency of the Raman and IR modes in a perovskite like framework [TPrA][Mn(dca)$_3$] was calculated depending on pressure for P-42$_1$C, Pcnb and P2$_1$/n phases by using the corresponding Eq. 4. Grüneisen values for ν_s(C≡N) (2244.4 cm^{-1}), ν_{as}(C≡N) (2158.1 cm^{-1}), δ(CNC) (844.7 cm^{-1}), ϱ(CH$_2$) (774.1 cm^{-1}) and T(dca)+L(dca)+T(Mn) (174.1 cm^{-1}) were used, and modes are shown in Figure 2.

The calculated frequency values for the interested internal modes tended to increase with increasing pressure, as expected for all structural phases. Also, these calculations are compatible with the experimental measurements by Mączka et al. (2019). Although there were not any significant jumps in the frequency measurements at 0.3 and 3.0 GPa for interested modes in [TPrA][Mn(dca)3], XRD, volume and dielectric measurements with pressure, other studies have shown a soft structural phase transition from P-421C to Pcnb at 0.3 GPa, and a distinct structural phase transition from Pcnb to P21/n at approximately 3.0 GPa (Bermúdez-García et al., 2015, 2017a, 2017b, 2018; Mączka et al., 2019). Results of the current study show that pressure significantly influences the lattice structure and electronic configuration of perovskite-like framework, as well as the ordering of molecular orientation in

[TPrA][Mn(dca)3]. In addition, the rise in Raman frequencies of the interested modes is likely directly correlated with the applied pressure. Although the phase transition at 0.3 and 3 GPa could not be clearly seen from Raman frequency measurements, Grüneisen values calculated with Eq. (3) show that there were obvious phase transitions at these pressure values, as in the literature, and as also shown in Figure 3.

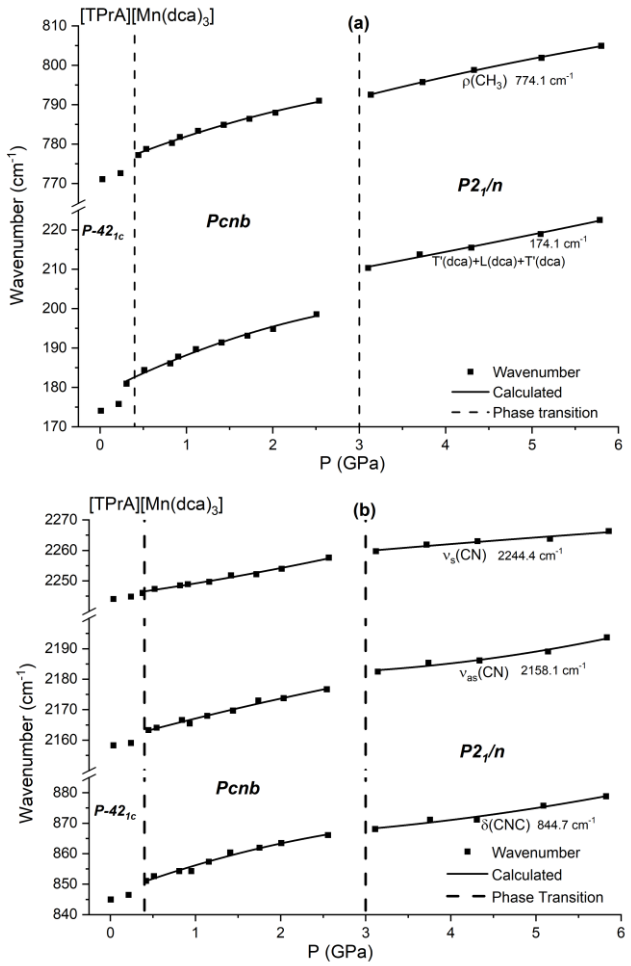

Figure 2. Calculated and observed (Mączka et al., 2019) frequency data of ν_s(C≡N), ν_{as}(C≡N), δ(C-NC), ϱ(CH2) and T(dca)+L(dca)+T(Mn) for P-42$_1$c, Pcnb and P2$_1$/n phases in [TPrA][Mn(dca)3].

As explained in detail above, the Grüneisen value is usually used to connect microscopic structure to macroscopic measurements, so the calculated Grüneisen values as a function of pressure really demonstrate these phase transitions for all internal modes (Figure 3). For ν_s(C≡N) (2244.4 cm^{-1}), ν_{as}(C≡N) (2158.1 cm^{-1}), δ(CNC) (844.7 cm^{-1}) and ϱ(CH$_2$) (774.1 cm^{-1}) internal modes in [TPrA][Mn(dca)$_3$], the calculated Grüneisen value almost exhibited a similar tendency with increasing pressure; however, the T(dca)+L(dca)+T(Mn) (174.1 cm^{-1}) IR mode had a very distinct trend. The cause of this behaviour for T(dca)+L(dca)+T(Mn) IR mode might be interference of the three bonds and energy exchange between these three modes.

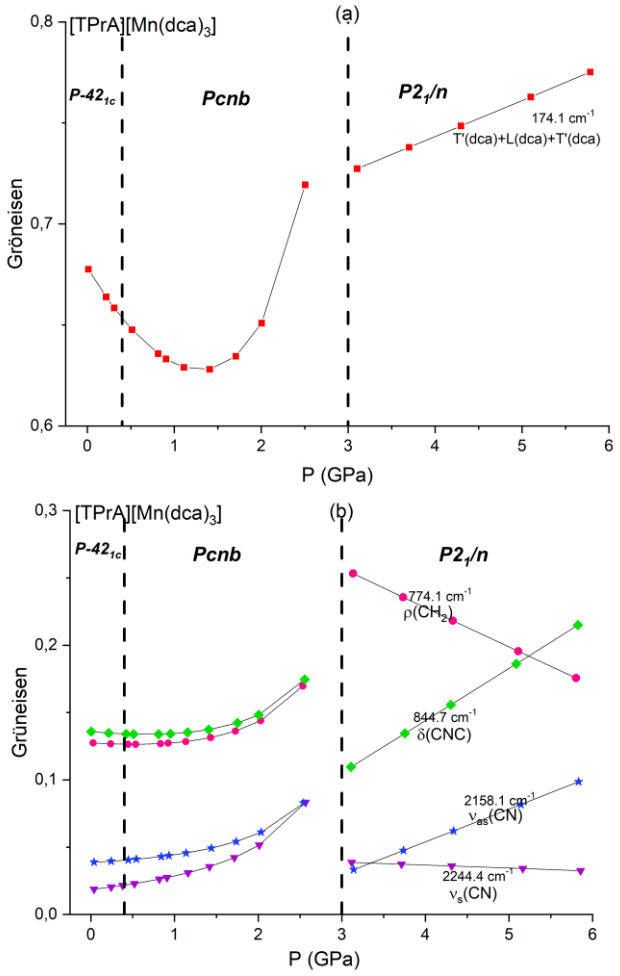

Figure 3. Calculated Isothermal Grüneisen values of ν_s(C≡N), ν_{as}(C≡N), δ(CNC), ϱ(CH$_2$) and T(dca)+L(dca)+T(Mn) for P-42$_1$c, Pcnb and P2$_1$/n phases in [TPrA][Mn(dca)$_3$].

The compressibility of a material defines the rate at which its volume alters in reaction to a change in pressure and is also crucial in the manufacturing of perovskite type solar panel cells, as it is for all solid materials. Perovskite materials with a high compressibility value are preferred in PV production processes because they easily modify the crystal structure with pressure (Kurt, 2022). In this study, the pressure-dependent compressibility for a perovskite-like framework of [TPrA][Mn(dca)$_3$] was also calculated by using Eq. 8 to determine how convenient it would be for the solar panel cell production. As seen

in Figure 4, the compressibility decreased up to 3 GPa but was almost constant after this pressure. However, no jump or discontinuity was seen at 0.3 GPa. This behaviour of isothermal compressibility shows that [TPrA][Mn(dca)$_3$] was in ordered phase up to ~3 GPa, after which a cell distortion to monoclinic symmetry occurred.

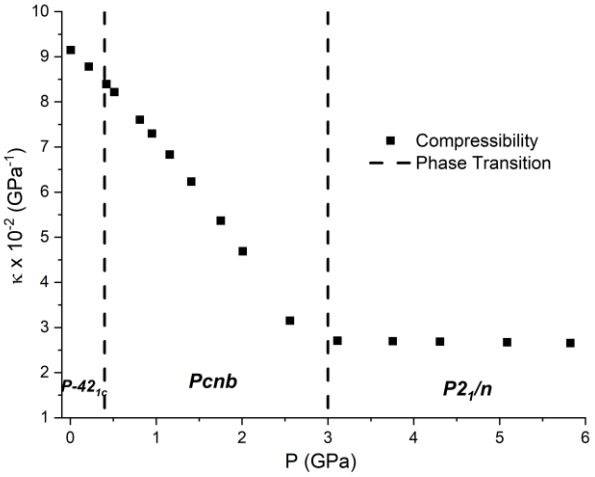

Figure 4. Calculated the isothermal compressibility κ_T by using Eq. (8) for P-42$_1$C, Pcnb and P2$_1$/n phases in [TPrA][Mn(dca)3].

Lastly, the isothermal bulk modulus was calculated depending on pressure through calculated isothermal compressibility for P-42$_1$C, Pcnb and P21/n phases (Figure 5.), also reported in Table 3. Mączka et al. (2019) determined the isothermal bulk modulus by fitting a 2nd order Birch–Murnaghan equation of state (EoS) to the volume–pressure dependence for Pcnb phase in their previous work. Their calculated value for this phase was 8.1 GPa and was almost the same as the calculated value (9.8 GPa) in the current study using Eq. 9 (Table 3). The isothermal bulk modulus was also determined with Eq. 9 for P-42$_1$C phase in [TPrA][Mn(dca)$_3$] and calculated as 36.0 GPa. Although this calculated value is a bit lower than 95 GPa for silicone, which is usually used in solar panel cell production, it is considerably larger than other perovskite materials that are candidates for solar panel cells. Results confirm that the perovskite-like framework of [TPrA][Mn(dca)$_3$] is a good material for new solar panel technology in the future.

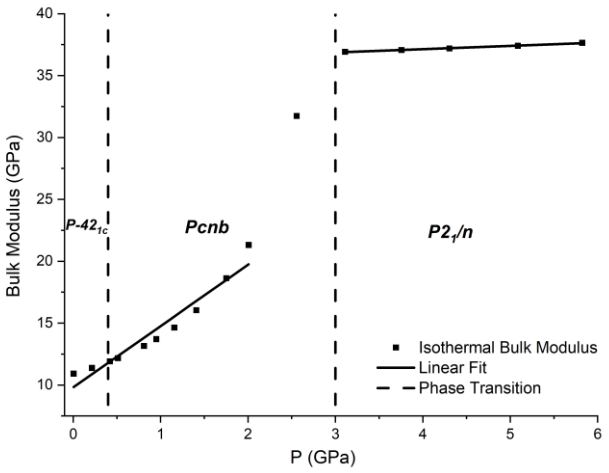

Figure 5. The isothermal Bulk modulus as a function of pressure, calculated by using Eq. (9) using the values of the isothermal compressibility (κ_T) for P-42$_1$C, Pcnb and P2$_1$/n phases in [TPrA][Mn(dca)$_3$]. A linear regression with coefficients (K_0) and (K_0') is shown by a straight line, as presented in Table 3.

CONCLUSION

For this study, we calculated Grüneisen values and isothermal compressibility as a function of pressure for ν_s(C≡N) (2244.4 cm^{-1}), ν_{as}(C≡N) (2158.1 cm^{-1}), δ(CNC) (844.7 cm^{-1}) and ϱ(CH2) (774.1 cm^{-1}) Raman modes in a perovskite-like framework of [TPrA][Mn(dca)$_3$]. We used the observed volume and Raman and IR mode frequency data close to the area where phase transitions occurred (P=0.3 and 3.0 GPa). In addition, we ascertained the Bulk modulus by using calculated isothermal compressibility for this perovskite. The calculated isothermal compressibility and Bulk modulus confirmed potential applications of the perovskite-like framework of [TPrA][Mn(dca)3] in high performance perovskite solar cells, light-emitting diodes, and photonic devices, making it a good candidate material for new solar panel technologies in the future. Our results also suggest that the calculated thermodynamic parameters are similar to those found in other studies, and our method of calculating these parameters can be used for additional perovskite-like frameworks with ferroelectric characteristics.

ACKNOWLEDGEMENTS

This study is part of PhD Thesis of the first author, and supported by Çanakkale Onsekiz Mart University the Scientific Research Coordination Unit, (Project number: FDK-2021-3591). Part of this study was presented at 3rd Global Conference on Engineering Research, 13-16 September 2023, Balıkesir, Türkiye.

Compliance with Ethical Standards

Authors' Contributions

Both authors have contributed equally to the paper. All authors read and approved the final manuscript.

Conflict of Interest

The authors declare that there is no conflict of interest.

Ethical Approval

For this type of study, formal consent is not required.

Data Availability

The data that support the findings of this study are available from the corresponding author upon request.

REFERENCES

Agyei-Tuffour, B., Doumon, N. Y., Rwenyagila, E. R., Asare, J., Oyewole, O. K., Shen, Z., Petoukhoff, C. E., Zebaze Kana, M. G., Ocarroll, D. M., & Soboyejo, W O. (2017). Pressure effects on interfacial surface contacts and performance of organic solar cells. *Journal of Applied Physics, 122*(20), 205501. https://doi.org/10.1063/1.5001765

Agyei-Tuffour, B., Rwenyagila, E. R., Asare, J., Oyewole, O. K., Zebaze Kana, M. G., O'Carroll, D. M., & Soboyejo, W. O. (2016). Influence of pressure on contacts between layers in organic photovoltaic cells. *Advanced Materials Research, 1132*, 204-216. https://doi.org/10.4028/www.scientific.net/AMR.1132.204

Assirey, E. A. R. (2019). Perovskite synthesis, properties and their related biochemical and industrial application. *Saudi Pharmaceutical Journal, 27*(6), 817-829. https://doi.org/10.1016/j.jsps.2019.05.003

Bermúdez-García, J. M., Sánchez-Andújar, M., Yáñez-Vilar, S., Castro-García, S., Artiaga, R., López-Beceiro, J., Botana, L., Alegría, Á., & Señarís-Rodríguez, M. A. (2015). Role of temperature and pressure on the multisensitive multiferroic dicyanamide framework [TPrA][Mn(dca)$_3$] with perovskite-like structure. *Inorganic Chemistry, 54*(24), 11680-11687. https://doi.org/10.1021/acs.inorgchem.5b01652

Bermúdez-García, J. M., Sánchez-Andújar, M., Castro-García, S., López-Beceiro, J., Artiaga, R., & Señarís-Rodríguez, M. A. (2017a). Giant barocaloric effect in the ferroic organic-inorganic hybrid [TPrA][Mn(dca)$_3$] perovskite under easily accessible pressures. *Nature Communications, 8*(1), 15715. https://doi.org/10.1038/ncomms15715

Bermúdez-García, J. M., Sánchez-Andújar, M., & Señarís-Rodríguez, M. A. (2017b). A new playground for organic–inorganic hybrids: Barocaloric materials for pressure-induced solid-state cooling. *The Journal of Physical Chemistry Letters, 8*(18), 4419-4423. https://doi.org/10.1021/acs.jpclett.7b01845

Bermúdez-García, J. M., Yáñez-Vilar, S., García-Fernández, A., Sánchez-Andújar, M., Castro-García, S., López-Beceiro, J., Artiaga, R., Dilshad, M., Moya, X., & Señarís-Rodríguez, M. A. (2018). Giant barocaloric tunability in [($CH_3CH_2CH_2$)$_4$N]Cd[$N(CN)_2$]$_3$ hybrid perovskite. *Journal of Materials Chemistry C, 6*(37), 9867-9874. https://doi.org/10.1039/C7TC03136J

Einstein, A. (1907). Die Plancksche Theorie der Strahlung und die Theorie der spezifischen wärme. *Annalen der Physik, 327*(1), 180-190. https://doi.org/10.1002/andp.19063270110

Grinberg, I., West, D. V., Torres, M., Gou, G., Stein, D. M., Wu, L., Chen, G., Gallo, E. M., Akbashev, A. R., Davies, P. K., Spanier, J. E., & Rappe, A. M. (2013). Perovskite oxides for visible-light-absorbing ferroelectric and photovoltaic materials. *Nature, 503*(7477), 509-512. https://doi.org/10.1038/nature12622

Grüneisen, E. (1912). Theorie des festen Zustandes einatomiger Elemente. *Annalen der Physik, 344*(12), 257-306. https://doi.org/10.1002/andp.19123441202

Huang, J., Yuan, Y., Shao, Y., & Yan, Y. (2017). Understanding the physical properties of hybrid perovskites for photovoltaic applications. *Nature Reviews Materials, 2*(7), 17042. https://doi.org/10.1038/natrevmats.2017.42

Jošt, M., Kohnen, E., Al-Ashouri, A., Bertram, T., Tomšič, Š., Magomedov, A., Kasparavicius, E., Kodalle, T., Lipovšek, B., Getautis, V., Schlatmann, R., Kaufmann, C. A., Albrecht, S., & Topič, M. (2022). Perovskite/CIGS tandem solar cells: from certified 24.2% toward 30% and beyond. *ACS Energy Letters, 7*(4), 1298-1307. https://doi.org/10.1021/acsenergylett.2c00274

Kurt, A. (2020). Pressure dependence of the Raman modes for orthorhombic and monoclinic phases of $CsPbI_3$ at room temperature. *Journal of Applied Physics, 128*(7), 075106. https://doi.org/10.1063/5.0012355

Kurt, A. (2022). Calculation of Gruneisen parameter, compressibility, and bulk modulus as functions of pressure in $(C_6H_5CH_2NH_3)_2PBI_4$. *Çanakkale Onsekiz Mart University Journal of Advanced Research in Natural and Applied Sciences, 8*(1), 63-75. https://doi.org/10.28979/jarnas.1003367

Li, Q., Zhang, L., Chen, Z., & Quan, Z. (2019). Metal halide perovskites under compression. *Journal of Materials Chemistry A, 7*(27), 16089-16108. https://doi.org/10.1039/C9TA04930D

Mączka, M., Collings, I. E., Leite, F. F., & Paraguassu, W. (2019). Raman and single-crystal X-ray diffraction evidence of pressure-induced phase transitions in a perovskite-like framework of $[(C_3H_7)_4N]$ $[Mn(N(CN)_2)_3]$. *Dalton Transactions, 48*(25), 9072-9078. https://doi.org/10.1039/C9DT01648A

Min, H., Lee, D. Y., Kim, J., Kim, G., Lee, K. S., Kim, J., Paik, M. J., Kim, Y. K., Kim, K. S., Kim, M. G., Shin, T. J., & Seok, S. I. (2021). Perovskite solar cells with atomically coherent interlayers on SnO_2 electrodes. *Nature, 598*(7881), 444-450. https://doi.org/10.1038/s41586-021-03964-8

Oyelade, O. V., Oyewole, O. K., Oyewole, D. O., Adeniji, S. A., Ichwani, R., Sanni, D. M., & Soboyejo, W. O. (2020). Pressure-assisted fabrication of perovskite solar cells. *Scientific Reports, 10*(1), 7183. https://doi.org/10.1038/s41598-020-64090-5

Shen, Z., Wang, X., Luo, B., & Li, L. (2015). $BaTiO_3$–$BiYbO_3$ perovskite materials for energy storage applications. *Journal of Materials Chemistry A, 3*(35), 18146-18153. https://doi.org/10.1039/C5TA03614C

Stacey, F. D., & Hodgkinson, J. H. (2019). Thermodynamics with the Grüneisen parameter: Fundamentals and applications to high pressure physics and geophysics. *Physics of the Earth and Planetary Interiors, 286*, 42-68. https://doi.org/10.1016/j.pepi.2018.10.006

Tan, J. C., & Cheetham, A. K. (2011). Mechanical properties of hybrid inorganic–organic framework materials: Establishing fundamental structure–property relationships. *Chemical Society Reviews, 40*(2), 1059-1080. https://doi.org/10.1039/C0CS00163E

Wang, W., Tadé, M. O., & Shao, Z. (2015). Research progress of perovskite materials in photocatalysis-and photovoltaics-related energy conversion and environmental treatment. *Chemical Society Reviews, 44*(15), 5371-5408. https://doi.org/10.1039/C5CS00113G

Xiao, G., Cao, Y., Qi, G., Wang, L., Liu, C., Ma, Z., Yang, X., Sui, Y., Zheng, W., & Zou, B. (2017). Pressure effects on structure and optical properties in cesium lead bromide perovskite nanocrystals. *Journal of the American Chemical Society, 139*(29), 10087-10094. https://doi.org/10.1021/jacs.7b05260

Xiao, G., Zhu, C., Ma, Y., Liu, B., Zou, G., & Zou, B. (2014). Unexpected room-temperature ferromagnetism in nanostructured Bi_2Te_3. *Angewandte Chemie International Edition, 53*(3), 729-733. https://doi.org/10.1002/anie.201309416

Yurtseven, H., & Cebeci, A. (2015). Pressure dependence of the Raman modes related to the phase transitions in cyclohexane. *Acta Physica Polonica A, 127*(3), 744-747. https://doi.org/10.12693/aphyspola.127.744

Yurtseven, H., & Kurt, M. (2011). Pressure dependence of the Raman frequency shifts related to the thermodynamic quantities in phase II of s-triazine. *Indian Journal of Physics, 85*, 615-628. https://doi.org/10.1007/s12648-011-0064-0

Yurtseven, H., & Ünlü, D. (2015). Temperature and pressure effect on the Raman frequencies calculated from the crystal volume in the γ-phase of solid nitrogen. *Journal of Applied Spectroscopy, 82*(4), 700-704. https://doi.org/10.1007/s10812-015-0166-0